remote sensing

Article

Retrieval of Aerosol Properties for Fine/Coarse Mode Aerosol Mixtures over Beijing from PARASOL Measurements

Shupeng Wang [1], Li Fang [2],*, Xingying Zhang [1] and Weihe Wang [1]

[1] National Satellite Meteorological Center, Beijing 100081, China; E-Mails: wangsp@cma.gov.cn (S.W.); zxy@cma.gov.cn (X.Z.); wangwh@cma.gov.cn (W.W.)

[2] Institute of Remote Sensing and Digital Earth, Chinese Academy of Sciences, Beijing 100101, China

* Author to whom correspondence should be addressed; E-Mail: fangli@radi.ac.cn; Tel./Fax: +86-10-6840-6617.

Abstract: Beijing is one of the largest metropolitan areas in the world with relatively high aerosol loading. The population of Beijing is approximately 21.5 million based on statistics from 2014. In order to improve the air quality of Beijing by monitoring and better understanding of high aerosol loading at fine spatial resolution, an extended version of the Look Up Table (LUT) aerosol retrieval algorithm from PARASOL (Polarization and Anisotropy of Reflectances for Atmospheric Science coupled with Observations from a Lidar) measurements of total intensity and polarization was tested over this region. Instead of using the surface reflectance model introduced in the GRASP (Generalized Retrieval of Aerosol and Surface Properties) algorithm, the assumption of spectral reflectance shape invariance principle is used to separate the total radiance contribution of surface and aerosols. Case studies were conducted in Beijing and evaluated preliminarily using the coincident AERONET measurements. The results indicate a significant agreement with a slope of 1.083 and a correlation coefficient of 0.913. A high Gfrac (fraction of accurate retrievals) of 78% is also observed. Analysis on the retrieval accuracy illustrates that the algorithm capability depends significantly on the data quality index, as the AOD (Aerosol Optical Depth) retrieval accuracy is relatively lower for the data with quality index less than 0.75.

Keywords: PARASOL; AERONET; fine/coarse aerosol mixture; aerosol retrieval; urban areas

1. Introduction

Radiative forcing caused by aerosols is thought to be one of the largest uncertainties in the radiative forcing of the earth's climate [1]. Both the direct scattering of shortwave solar radiation and the enhancement on brightness of clouds caused by increased concentration of cloud condensation nuclei are identified to exert a cooling influence on the planet [2–4]. The aerosol radiative influence represents a larger uncertainty in climate change research than forcing by greenhouse gases [5]. However, the level of scientific understanding of aerosol radiative forcing remains very low [6]. Better estimates of the perturbations to earth's radiation budget require accurate optical and physical properties of aerosols such as spectral aerosol optical depth (AOD, ±0.02), size distribution (effective radius ±10%, effective variance ±40%) and single scattering albedo (SSA, ±0.03) [7,8]. Daily determination of these parameters on a global scale can be achieved by means of satellite remote sensing. Orbital remote sensing instruments that perform multi-angle, multi- spectral photopolarimetric measurements have the capability to provide these aerosol properties with the required accuracy [9,10]. The advantages of polarimetric measurements over intensity-only measurements come from the sensitivity of polarization of light and its spectral and angular dependence to particle size, shape, and refractive index [7,11].

PARASOL (Polarization and Anisotropy of Reflectances for Atmospheric Science coupled with Observations from a Lidar), the most recent in-orbit polarization measuring satellite instrument, performed multi-spectral, multidirectional, and polarized measurements over daily global coverage by a swath of 1600 km cross track [12,13]. The usage of LUT (Look Up Table) for aerosol properties retrieval has been conducted in many earlier studies [14,15]. The operational land aerosol inversion strategy, detailed in [16], is also based on the LUT approach, where the polarized reflectances are simulated for 10 aerosol models (log-normal size distributions) with effective radius from 0.075 to 0.225 μm and a mean refractive index $m = 1.47 − 0.01i$. The aerosol parameters are adjusted to give the best agreement between the measured and simulated multi-directional polarized radiances at 0.670 and 0.865 μm. However, since the sunlight scattered by the small particles is highly polarized while coarse-mode aerosols polarize very little, only the fine mode can be retrieved.

The GRASP (Generalized Retrieval of Aerosol and Surface Properties) algorithm is an attempt to enhance aerosol retrieval by emphasizing statistical optimization using the data redundancy available from advanced satellite observations [17]. The algorithm fits the complete set of POLDER/PARASOL observations in all spectral channels (except 763, 765, and 910 nm dominated by gaseous absorption) for up to 16 observation geometries including both measurements of total radiances and linear polarization. Based on this strategy, the algorithm aims at retrieval of an extended set of aerosol microphysical parameters including the aerosol volume size distribution (in bins), the total volume concentration of aerosol, the complex aerosol refractive index, mean height of aerosol layer, and the fraction of nonspherical scatterers. Then these retrieved parameters are used to calculate the total aerosol optical thickness, single scattering albedo, and aerosol phase matrix. Also, the approach allows for the retrieval of surface reflectance parameters.

The SRON (Netherlands Institute for Space Research) algorithm fits POLDER observations at selected wavelengths and observation geometries simultaneously [18]. The algorithm derives the following parameters: the effective radius, the effective variance, the refractive index (assumed to be spectrally neutral) in both modes, and also AODs for the fine and coarse modes. The algorithm is based

on direct radiative transfer calculations during the retrieval process. The derivatives are calculated using the solution of the adjoining radiative transfer equation. The Tikhonov regularization method is used in the retrieval process.

In this work an extended version of the LUT aerosol retrieval algorithm [16] from PARASOL measurements of total intensity and polarization is presented to retrieve aerosol properties for fine/coarse mode aerosol mixtures over Beijing, China. Beijing is one of the largest metropolitan areas in the world. Studies have demonstrated that the aerosol loading is extremely high in the urban areas of Beijing [19,20]. Traditionally, the major particle emission sources consist of industrial emissions, coal burning for winter heating and power supply, and long-range transported dust. In recent years, traffic emission has become a major contributor to the severe air pollution in Beijing, making the particle composition more complex and variable [21]. In addition, because of the rapid economic growth and urbanization, air pollution has become a serious problem for Beijing. Urbanization has been also found to have adverse effects on greenhouse gases and air quality degradation over other megacities in the world [22,23]. Since the 1990s, several pollution-control measures have been deployed in Beijing, such as natural gas substitution for coal and the use of low-sulfur coal. However, inhalable particles (PM10, particles smaller than 10 μm in aerodynamic diameter) pollution is still at a level higher than the Chinese national ambient air quality standard. In order to improve the air quality of Beijing by monitoring and better understanding of high aerosol loadings at fine spatial resolution, the algorithm was tested over the urban areas of Beijing.

Different from the LOA (Laboratoire d'Optique Atmosphérique)-LUT algorithm, the total intensity measurements of PARASOL are used to retrieve the AOD contribution of coarse mode particles. Instead of using the surface reflectance model introduced in the GRASP algorithm, the assumption of spectral reflectance shape invariance principle [24] is used to separate the total radiance contribution of surface and aerosols. Section 2 presents the retrieval approach and the sensitivity analysis of the assumption. Section 3 gives a description of the study area, AERONET instrumentation, and methodology, as well as the aerosol models. Section 4 looks in detail at the performance of the algorithm in Beijing, China. Finally, conclusions are presented in the last section.

2. Retrieval Principle and Method

2.1. The Assumption of the Spectral Reflectance Shape Invariance Principle

The spectral reflectance shape invariance principle was first developed by Flowerdew and Haigh, 1995 [24], which suggested that the shape of the surface Hemispherical Directional Reflectance Factor (HDRF) should be nearly spectrally invariant because the surface scattering elements are much larger than the wavelengths of the scattered light. Aerosol retrieval algorithms based on this idea using ATSR-2 (Along-Track Scanning Radiometer successor instruments) dual-look data demonstrated good agreement with ground-based sunphotometer measurements [25,26]. On this assumption, proper aerosol optical thickness and aerosol model, which lead to the minimum spectral variance of angle-averaged HDRFs, can be selected from the LUT.

In the case of PARASOL, the spatially averaged HDRF over the 3×3 array of 6.7-km sub-regions can be approximately expressed as:

$$\rho_\lambda(\mu_s, -\mu_v, \Delta\varphi) = \frac{L_\lambda^{\text{meas}}(\mu_s, -\mu_v, \Delta\varphi) - L_\lambda^{\text{atm}}(\mu_s, -\mu_v, \Delta\varphi)}{[\exp(-\tau_\lambda/\mu_v) + t_\lambda^{\text{diff}}(-\mu_v)] \times L_\lambda^{\text{surf}}(\mu_s)} \qquad (1)$$

Where L_λ^{means} is the TOA (Top Of Atmosphere) radiance, L_λ^{atm} is the atmospheric path radiance, τ_λ is the total atmospheric optical depth, t_λ^{diff} is the upward diffuse, azimuthally integrated, atmospheric transmittance, and L_λ^{surf} is the downwelling normalized illumination at the surface level .

Dividing ρ_λ by the angular average value $\langle\rho_\lambda\rangle_{\text{dir}}$, this normalized HDRF, $\rho_{\text{dirnorm, }\lambda}$ is given by

$$\rho_{\text{dirnorm},\lambda}(i) = \frac{\rho_\lambda(i)}{\langle\rho_\lambda(i)\rangle_{\text{dir}}} = \frac{[L_\lambda^{\text{meas}}(i) - L_\lambda^{\text{atm}}(i)]/[\exp(-\tau_\lambda/\mu_i) + t_\lambda^{\text{diff}}(i)]}{\langle[L_\lambda^{\text{meas}} - L_\lambda^{\text{atm}}]/[\exp(-\tau_\lambda/\mu) + t_\lambda^{\text{diff}}]\rangle_{\text{dir}}} \qquad (2)$$

where the explicit imaging geometry, $\mu_s, -\mu_v, \Delta\varphi$, is replaced by the angular index *i*. All the atmospheric parameters in this equation are pre-calculated for the predetermined aerosol models using RT3 vector radiative transfer model, which simulates radiation fields in the atmosphere-land system, assuming plane parallel atmosphere [27].

For a given aerosol model the wavelength independence condition may be measured by means of a fit function, X_{angular}^2, defined as

$$X_{\text{angular}}^2(\tau_a, \text{model}) = \frac{\sum_\lambda w_\lambda \left\{\sum_i q_i[\rho_{\text{dirnorm},\lambda}(i) - \langle\rho_{\text{dirnorm}}(i)\rangle_\lambda]^2\right\}}{(0.05)^2 \sum_\lambda w_\lambda \sum_i q_i} \qquad (3)$$

where $\langle\rho_{\text{dirnorm}}\rangle_\lambda$ is the spectral band average of $\rho_{\text{dirnorm, }\lambda}$, w_λ are band weights and q_i are -angular weights. As implemented, bands of blue, green, red, and near-IR are assigned w_λ values of 4, 3, 2, and 1, respectively, indicating higher weights for the shorter wavelengths. Similarly, the angular weights, q_i, are set to the view angle reciprocal cosine, $1/\mu_v$, taking advantage of the greater atmospheric sensitivity in the oblique views.

The aerosol model and optical depth that minimize Equation (3), in principle, would be the 'best estimation' of the actual aerosol conditions. In the retrieval progress, the usage of spectral reflectance shape invariance principle is to obtain possible aerosol mode and optical properties. The aerosol models and optical depths satisfying $X_{\text{angular}} < 2$ are retained as possible solutions to the retrieval process.

2.2. Sensitivity Study of the Assumption

To test whether the assumption of spectral reflectance shape invariance principle is suitable for the spatial resolution of PARASOL, PARASOL observations with low aerosol loading on 26 October 2009 over Beijing (39.99 °N, 116.38 °E) and Xianghe (39.75 °N, 116.96 °E) with high and relatively low surface heterogeneity, respectively, are used to calculate the normalized HDRFs defined in Equation (2). The required aerosol optical properties are obtained from AERONET near the overpass time of PARASOL. The AOD at 870 nm over Beijing and Xianghe AERONET sites on 26 October 2009 was 0.061 and 0.083, respectively. With the obtained AOD and aerosol microphysical parameters, we use RT3 radiative transfer codes to calculate the atmospheric path radiance and transmittance required in Equation (2); thus, the normalized HDRF at different bands can be calculated. Then the standard deviation of different bands can also be calculated.

Figure 1a,b shows HDRF normalized by the average over angle for Xianghe and Beijing, respectively. Let δ_{iangle} be the standard deviation for each view zenith angle, and $\text{HDRF}_{\text{iangle}}^m$ be the mean normalized

HDRF of four wavelengths; the average of $\delta_{\text{iangle}}/\text{HDRF}^m_{\text{iangle}}$ over different zenith angles are smaller than 5% (4.9% for Xianghe and 3.2% for Beijing). The different spectral normalized HDRFs of both sites show spectral similarity. The normalized HDRF of Xianghe shows a larger standard deviation than that of Beijing because of less surface heterogeneity in Xianghe. The conclusion of less vegetation and larger surface heterogeneity leading to smaller standard deviation of normalized HDRF is also shown by Diner *et al.*, (2005) [28]. These results demonstrate that, despite a strong spectral variation in reflectance factor from the visible to the near-infrared, the relative angular shapes of the HDRFs are remarkably similar among the spectral bands, lending credence to the assumption.
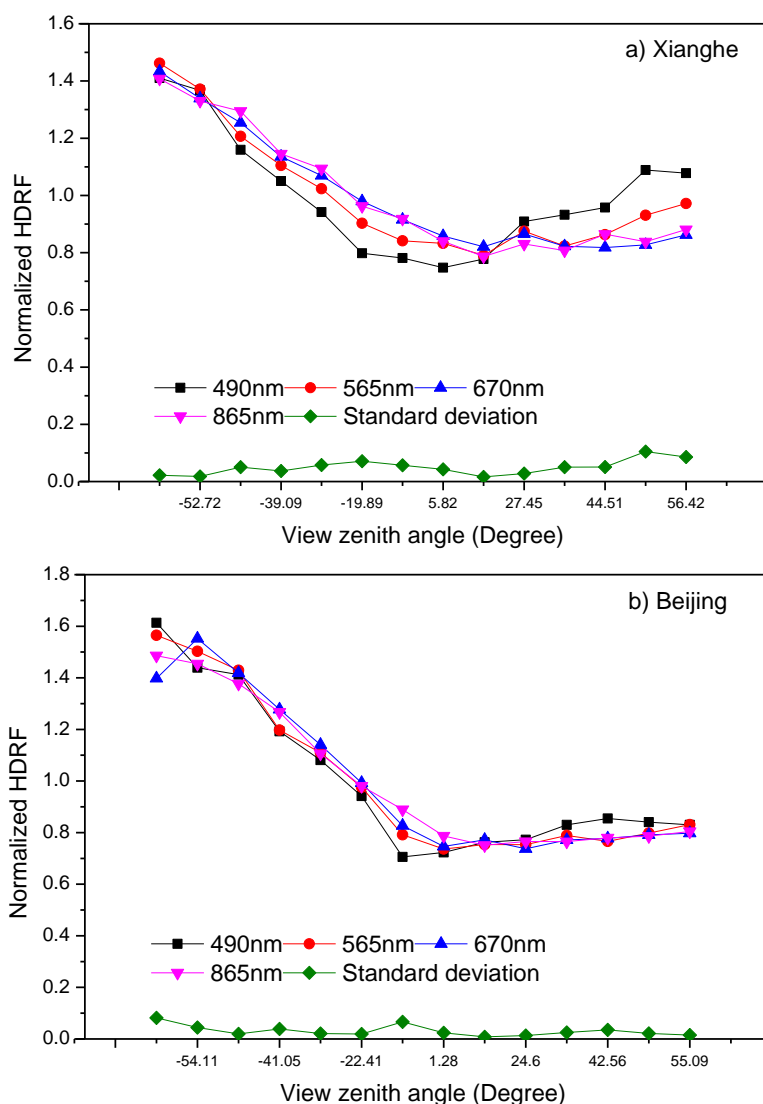

Figure 1. Normalized HDRFs and the corresponding standard deviation calculated from PARASOL intensity on 26 October 2009 over (**a**) Xianghe and (**b**) Beijing.

2.3. Aerosol Retrieval Process

Figure 2 gives the flowchart of the retrieval process. First, only cloud-free POLDER pixels are considered according to the cloud-screening algorithm of Bréon and Colzy (1999) [29]. Then, preliminary aerosol models and the corresponding AODs are obtained using the assumption of spectral reflectance shape invariance principle.
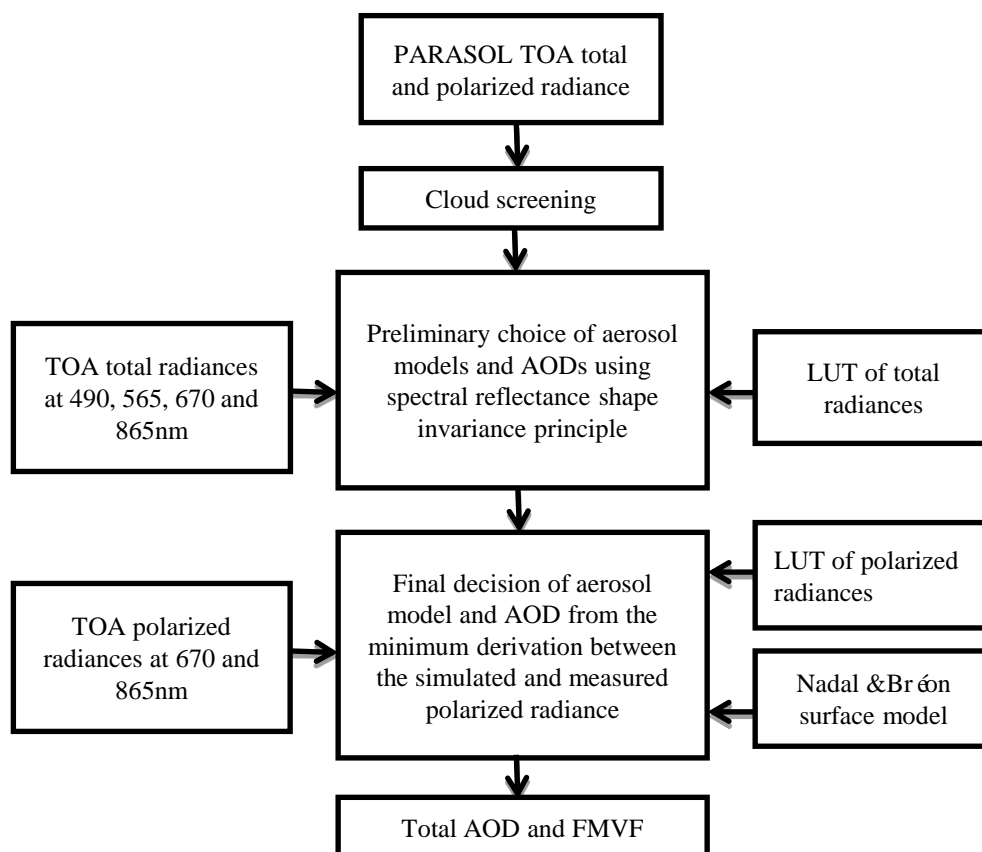
Figure 2. The flowchart of the aerosol retrieval process from PARASOL total and polarized radiances.

With the possible aerosol models and AODs obtained previously, the multi-angle polarized reflectances at 670 nm and 865 nm can be obtained using the LUT constructed previously. The minimum derivation between the simulated polarized radiance and the measured polarized radiance lead to the final decision on the total AOD and FMVW (Fine Mode Volume Weighting), defined as the percentage of the fine mode volume concentration in the total volume concentration.

The LUTs of TOA polarized reflectance at 670 nm and 865 nm are constructed using an RT3 vector radiative transfer model. The surface BPDF (Bidirectional Polarization Distribution Functions) model of Nadal and Bréon (1999) [30], based on Normalized Difference Vegetation Index classification, was used to estimate the polarized reflectance. The aerosol models for the study area are described in Section 3.2.

3. Data Processing

3.1. Study Area Description

As the capital of China, Beijing (39.9 °N, 116.4 °E) is a mega-city with a population of approximately 21.5 million (based on statistics from 2014) and a population density of 1341 people/km^2. It is located along the northwestern border of the Great Plain of North China, surrounded by the Taihang Mountains to the west and the Yanshan Mountains to the north. Heavy aerosol emissions generated by fossil fuel combustion are present throughout the year, due to the rapid increase over the past two decades in both economic activities and the number of vehicles on the road. In spring, desert dust advected from the Kumutage and Taklamakan deserts west of Beijing and from Mongolian deserts north of Beijing blankets

the city and mixes with local aerosols. Summer is the rainy season and accounts for about 74% of the annual precipitation [31]. Increased amounts of fine-mode pollution from combustion are seen in winter, which is the season when artificial heating is used. Seasons in Beijing are defined according to the following months: March–May (spring), June–August (summer), September–November (autumn) and December–February (winter). Intensive investigation of the aerosol properties over Beijing from ground-based measurements by sunphotometers were given by several studies [19,32].

3.2. Aerosol Models

We assume that the aerosol population can be described by a bimodal size distribution [33]. Each mode (coarse and fine) is described by its own log-normal size distribution given by

$$\frac{\mathrm{d}V}{\mathrm{d}\ln r} = \frac{C_{\text{fine}}}{\sigma_{fine}\sqrt{2\pi}}\exp(-\frac{[\ln(r/R_{fine})]^2}{2\sigma_{fine}^2}) + \frac{C_{\text{coarse}}}{\sigma_{\text{coarse}}\sqrt{2\pi}}\exp(-\frac{[\ln(r/R_{\text{coarse}})]^2}{2\sigma_{\text{coarse}}^2}) \tag{4}$$

where C, R, and σ are volume concentration ($\mu m^3/\mu m^2$), particle radius (μm), and geometric standard deviation, respectively. R_{fine} and R_{coarse} denote mean radius for fine and coarse modes. This partition of the size distribution into fine and coarse modes yields six parameters by which the size distribution can be described. In the following, the suffixes *f* and *c* indicate parameters that belong to the fine and coarse mode, respectively.

In order to represent the average aerosol model for Beijing, the parameters of assumed aerosol models except for the FMVW are obtained by averaging AERONET retrievals at Beijing for five years from 2005 to 2009. The average aerosol volume size distribution is shown in Figure 3. Table 1 displays the complex refractive indices and size parameters for fine and coarse modes. Considering the increased amounts of desert dust in spring and fine-mode pollution in winter over Beijing, the fine and coarse aerosol modes were combined with several FMVW, *i.e.*, 20%, 30%, 40%, 50%, 60%, yielding five bimodal size distributions corresponding to a fine-dominated aerosol model or a coarse-dominated aerosol model, where FMVW is defined as $C_{\text{fine}}/(C_{\text{fine}} + C_{\text{coarse}})$.

In order to account for aerosol non-sphericity, the atmospheric aerosols are modeled as an ensemble of randomly oriented spheroids. Dubovik *et al.* (2006) developed a numerical tool for fast calculations of scattering properties of spheroid mixture [33]. The quadrature coefficients $K_{\text{ext}}^{\varepsilon}(\lambda; k; n; r_i; \varepsilon_k)$ for the extinction, as well as for absorption cross-sections and scattering matrices, have been calculated and stored into the look-up tables for a wide range of *n* and k values ($1.3 \leq n \leq 1.7$; $0.0005 \leq k \leq 0.5$). The calculations were done for spheroids with axis ratio ε ranging from ~0.3 (flattened oblate spheroids) to ~3.0 (elongated prolate spheroids) and for 41 narrow size bins covering the size-parameter range from ~0.012 to ~625. It was shown that scattering matrices have rather limited sensitivity to the minor details of axis ratio distribution. Therefore, Dubovik *et al*. (2006) have demonstrated that AERONET retrieval may rely on the rather simple assumption that the shape (axis ratio) distribution in the non-spherical fraction of any tropospheric aerosol is the same.

The algorithm uses LUT with the atmospheric parameters of Equation (1) pre-calculated from the RT3 radiative transfer model.
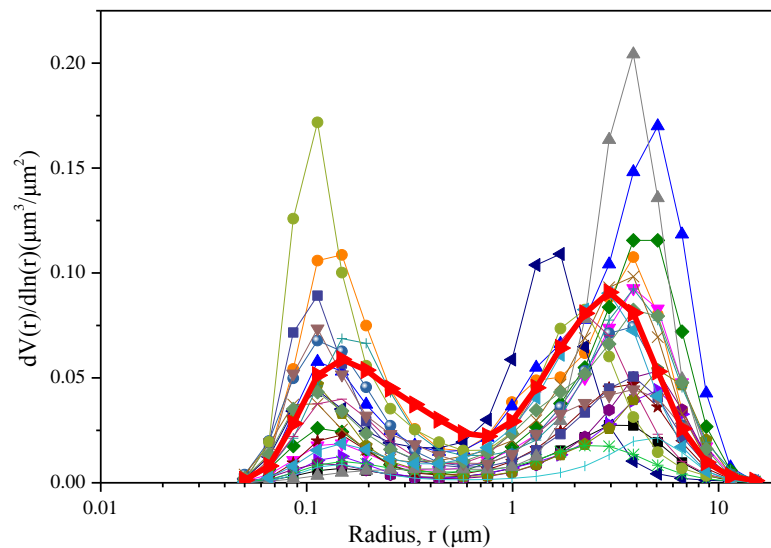
Figure 3. Aerosol volume size distributions of the 22 cases obtained from the closest AERONET retrievals within half an hour of satellite overpass for Beijing. The wider red line stands for the average size distribution from 2005 to 2009.

Table 1. Detailed parameters of the assumed aerosol models *.

Aerosol Mode	Fine Mode	Coarse Mode
R_v (μm)	0.182	2.705
σ	0.508	0.610
Effective radius (μm)	0.160	2.225
Real refractive index	B: 1.484; G:1.489; R: 1.497; N:1.506	
Imaginary refractive index	B:0.0121; G:0.0107; R:0.0086; N: 0.0092	
FMVW	20%, 30%, 40%, 50%, 60%	

* "B", "G", "R", and "N" denote the blue, green, red, and Near IR bands of PARASOL, respectively.

4. Validation and Discussion

To evaluate the performance of the regional algorithm, a comparison between the retrieved AOD with a resolution of ~20 km × 20 km over Beijing and AERONET sunphotometer data has been done. Validated datasets are obtained from AERONET measurements in Beijing [34,35]. For assessment of the AOD retrievals, the coincident measurements are considered for comparison. As the Level 2.0 retrievals close to satellite overpass time were generally not available, Level 1.5 retrievals are used to ensure enough match-ups for comparison. Moreover, to keep the atmospheric conditions stable for comparing satellite and ground-based data, the closest AERONET retrievals within half an hour of satellite overpass time are selected in this work. The wavelength is 550 nm. Therefore, the CE318 AOD data are transformed to AOD at 550 nm based on the Ångström exponent of aerosols provided by AERONET.

Figure 4 shows the comparison of the retrieved AODs from PARASOL against AERONET measurements. The two datasets indicate a significantly high correlation ($R = 0.913$) and a low root-mean-square-error (RMSE = 0.098) from the 22 collocations covering four seasons. The linear

regression slope of 1.083 with an intercept of 0.0074 suggests that the algorithm is promising for aerosol retrieval over the urban areas of Beijing.

Comparison of PARASOL AOD with ground-based sunphotometer measurements [36] demonstrated higher correlation and Gfrac (fraction of good retrievals) as the quality index Q increases (A significant correlation of 0.91 for $0.75 \leq Q \leq 1.0$, however a correlation of only 0.74 for $0.5 \leq Q \leq 0.75$), where a good retrieval was defined as being when the difference with the sunphotometer data is less than

$$\Delta\tau = 0.05 + 0.15\tau_{AERONET}, \tag{5}$$

where $\tau_{AERONET}$ is the aerosol optical depth measured by the AERONET sunphotometer.

We investigated the statistics as a function of the quality index. As PARASOL products provide two kinds of quality index, one for viewing geometry conditions and the other for polarized reflectance fit, the average, denoted by Q_{mean}, was used as the quality indicator in this study. The AOD retrieval error is defined as the relative difference against AERONET data:

$$\xi_{\tau_{retrived}^{total}} = (\tau_{retrieved} - \tau_{AERONET}) / \tau_{AERONET} \times 100\ \% \tag{6}$$

Table 2. Detailed information on the cases used for validation and discussion *.

Season	Date	Q_{mean}	τ_{AER}^{total}	$\tau_{retrieved}^{total}$	η_{AER}	$\eta_{retrieved}$	$\xi_{\tau_{retrived}^{total}}$
Spring	03/03/2006	0.850	0.781	0.92	45%	30%	17.8%
	06/03/2006	0.830	0.549	0.63	22%	20%	14.8%
	26/03/2008	0.725	0.235	0.42	16%	30%	78.7%
	05/03/2009	0.755	0.090	0.07	16%	20%	−22.2%
	17/05/2009	0.805	0.278	0.39	16%	20%	40.3%
Summer	17/06/2006	0.740	0.132	0.09	18%	20%	−31.8%
	04/06/2007	0.745	0.542	0.73	31%	30%	34.7%
	02/06/2009	0.780	0.094	0.13	14%	20%	38.3%
Autumn	21/10/2005	0.725	0.213	0.29	25%	50%	36.2%
	30/10/2005	0.595	0.069	0.15	28%	60%	117.4%
	20/11/2005	0.770	0.169	0.24	39%	60%	42.0%
	29/09/2006	0.790	0.429	0.32	30%	50%	−25.4%
	05/10/2009	0.770	0.398	0.49	44%	40%	23.1%
	06/10/2009	0.845	0.493	0.54	40%	30%	9.5%
	22/10/2009	0.775	0.256	0.28	25%	20%	9.4%
	26/10/2009	0.735	0.111	0.09	30%	20%	−18.9%
Winter	04/12/2005	0.710	0.182	0.11	6%	20%	−39.6%
	08/12/2005	0.795	0.477	0.42	51%	40%	−11.9%
	18/02/2006	0.830	0.391	0.18	28%	30%	−54.0%
	25/02/2006	0.805	0.273	0.30	15%	20%	9.9%
	28/11/2007	0.785	0.575	0.61	60%	40%	6.1%
	30/11/2008	0.745	0.225	0.30	54%	30%	33.3%

* "AER" denotes AERONET.

The retrieval error of FMVW can be analogously estimated. Detailed information on all the samples used for validation is reported in Table 2. The average AOD error of all cases is 14.0%, with the majority of retrievals falling within the good retrieval threshold defined above, resulting in a high Gfrac of 78%. The statistics show that our retrievals are clearly much better when Q_{mean} is greater. For the eight cases with $Q_{mean} < 0.75$, the average AOD retrieval error is 26.2% with a RMSE of 0.109 and the average retrieval error for the FMVW is 58.2%. When Q_{mean} is greater than 0.75, the average AOD retrieval error is 7.0% with the RMSE of 0.092 and the average retrieval error for the FMVW is 7.3%. The comparison between the two set of statistics indicates that our retrieval agreement with AERONET data depends very much on the quality index.
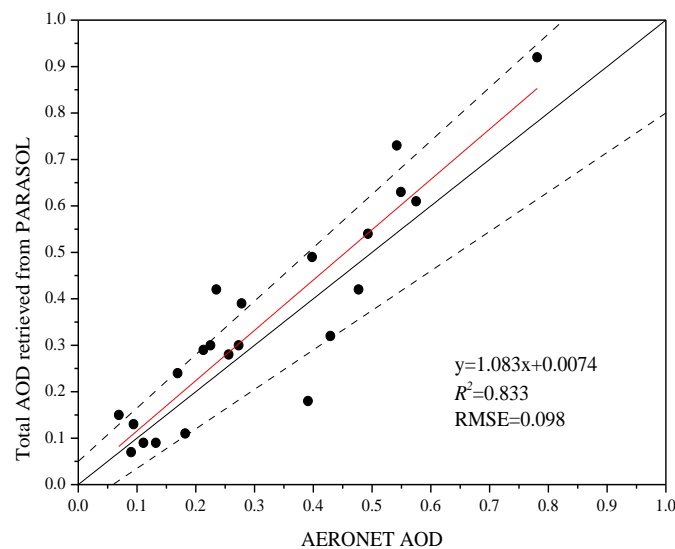

Figure 4. Comparison of AOD (550 nm) retrieved from PARASOL against AERONET sunphotometer measurements. The dash lines correspond to $\pm 0.05 \pm 0.15\tau_{AERONET}$ error of total AOD.
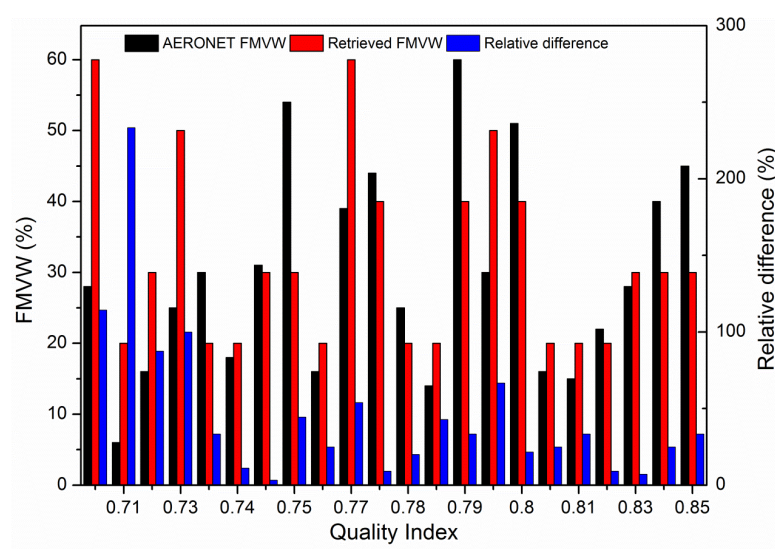

Figure 5. The variation of the FMVW retrieved from PARASOL, the FMVW obtained from AERONET, and the relative error as a function of the quality index. Note that the quality index (*X*-axis) is not displayed linearly, but corresponds to the values of the 22 samples.

Figure 5 illustrates the variation of the FMVW retrieved from PARASOL, the FMVW obtained from AERONET and the relative error as a function of the quality index Q_{mean}. The results show that the relative error stays at a low level for Q_{mean} greater than 0.75, while it varies in a much larger range for Q_{mean} less than 0.75. Though the correlation is higher for Q_{mean} greater than 0.75, the derived FMVW estimates show less resemblance to AERONET values, possibly arising from uncertainty in the prior aerosol models.

5. Conclusions

As the capital of China, Beijing is a mega-city with a population of 21.5 million and a population density of approximately 1340 people km^{-2}. In order to improve the air quality of Beijing by monitoring and better understanding of high aerosol loadings at fine spatial resolution, an extended version of the LUT aerosol retrieval algorithm was tested over the region and the retrieval results are evaluated preliminarily using the coincident AERONET data. The retrieval algorithm exploits the spectral reflectance shape invariance principle of multi-angle total radiances to preliminary constrain the choice of possible AODs and aerosol models. The retrieved aerosol parameters $\tau_{retrieved}^{total}$ and $\eta_{retrieved}$ (FMVW, Fine Mode Volume Weighting) correspond to the aerosol load and aerosol model that give the best agreement between the simulated and measured multi-angle polarized reflectances at 670 nm and 865 nm.

The comparison between the retrieved AOD with a resolution of ~20 km $\times$ 20 km over Beijing and AERONET sunphotometer measurements indicates a high correlation ($R = 0.913$) and a low root-mean-square-error (RMSE = 0.098). The average AOD retrieval error of all cases is 14.0% with the majority of retrievals falling within the good retrieval threshold described in [30], resulting in a high Gfrac of 78%. The linear regression slope of 1.083 with an intercept of 0.0074 suggests that the algorithm is very promising for aerosol retrieval over urban areas.

It is found from the statistics that our retrieval agreement with AERONET data depends significantly on the data quality index. For the cases with $Q_{mean} > 0.75$, the average AOD retrieval error and RMSE are obviously lower than those for the case when Q_{mean} is less than 0.75. Relatively larger retrieval error of FMVW can probably be attributed to the discrepancy between the pre-assumed and the true aerosol models.

Since the retrieval accuracy depends on the agreement between the aerosol mode used in the LUT and the real regional aerosol model, more typical aerosol modes will be included in the aerosol mode database. Also, the retrieval accuracy of the microphysical properties of aerosol such as SSA and refractive index will be evaluated in the following work.

Author Contributions

Shupeng Wang performed the aerosol algorithm research and prepared the paper. Li Fang contributed to the algorithm research and ground-based data collection. Xingying Zhang and Weihe Wang provided the technical guidance and contributed to the error discussion.

Conflicts of Interest

The authors declare no conflict of interest.

References

1. Intergovernmental Panel on Climate Change (IPCC). Climate change 2013: The physical science basis, intergovernmental panel on climate change. In *Working Group I Contribution to the IPCC Fifth Assessment Report* (*AR5*); Cam-bridge University Press: New York, NY, USA, 2013; p. 2794.
2. Nemesure, S.; Wagener, R.; Schwartz, S.E. Direct shortwave forcing of climate by the anthropogenic sulfate aerosol: Sensitivity to particle size, composition, and relative humidity. *J. Geophys. Res. Atmos.* **1995**, *100*, 26105–26116.
3. Hansen, J.; Sato, M.; Ruedy, R. Radiative forcing and climate response. *J. Geophys. Res.* **1997**, *102*, 6831–6864.
4. Ramanathan, V.; Crutzen, P.J.; Kiehl, J.T.; Rosenfeld, D. Atmosphere-aerosols, climate, and the hydrological cycle. *Science* **2001**, *294*, 2119–2124.
5. Hansen, J.; Nazarenko, L.; Ruedy, R.; Sato, M.; Willis, J.; Del Genio, A.; Koch, D.; Lacis, A.; Lo, K.; Menon, S.; *et al.* Earth's energy imbalance: Confirmation and implications. *Science* **2005**, *308*, 1431–1435.
6. Intergovernmental Panel on Climate Change (IPCC). Climate Change 2014: Synthesis Report. Available online: http://www.ipcc.ch/report/ar5/syr/ (accessed on 20 July 2014).
7. Mishchenko, M.; Cairns, B.; Kopp, G.; Schueler, C.F.; Fafaul, B.; Hansen, J.; Hooker, J.; Itchkawich, T.; Maring, H.; Travis, L.D. Accurate monitoring of terrestrial aerosols and total solar irradiance: Introducing the Glory Mission. *Bull. Am. Meteorol. Soc.* **2007**, *88*, 677–691.
8. Pal, S.; Devara, P.C.S. A wavelet-based spectral analysis of long-term time series of optical properties of aerosols obtained by Lidar and radiometer measurements over an urban station in Western India. *J. Atmos. Solar Terr. Phys.* **2012**, *84–85*, 75–87.
9. Mishchenko, M.I.; Travis, L.D. Satellite retrieval of aerosol properties over the ocean using polarization as well as intensity of reflected sunlight. *J. Geophys. Res. Atmos.* **1997**, *102*, 16989–17013.
10. Hasekamp, O.P.; Landgraf, J. Retrieval of aerosol properties over land surfaces: Capabilities of multiple-viewing-angle intensity and polarization measurements. *Appl. Opt.* **2007**, *46*, 3332–3344.
11. Kokhanovsky, A.A. The modern aerosol retrieval algorithms based on the simultaneous measurements of the intensity and polarization of reflected solar light: A review. *Front. Environ. Sci.* **2015**, *3*, doi:10.3389/fenvs.2015.00004.
12. Deschamps, P.Y.; Breon, F.M.; Leroy, M.; Podaire, A.; Bricaud, A.; Buriez, J.C.; Seze, G. The polder mission instrument characteristics and scientific objectives. *IEEE. Trans. Geosci. Remote Sens.* **1994**, *32*, 598–615.

13. Tanré, D.; Bréon, F.M.; Deuzé, J.L.; Dubovik, O.; Ducos, F.; Francois, P.; Goloub, P.; Herman, M.; Lifermann, A.; Waquet, F. Remote sensing of aerosols by using polarized, directional and spectral measurements within the A-Train: The PARASOL mission. *Atmos. Meas. Tech.* **2011**, *4*, 1383–1395.

14. Valdebenito, B.; Behrendt, A.; Pal, S.; Wulfmeyer, V.; Valdebenito A.M.B.; Lammel, G. A novel approach for the characterization of transport and optical properties of aerosol particles emitted from an animal facility—Part II: High-resolution chemistry transport model and its assessment using Lidar measurements. *Atmos. Environ.* **2011**, *45*, 2981–2990.

15. Behrendt, A.; Pal, S.; Wulfmeyer, V.; Valdebenito, A.M.B.; Lammel, G. A novel approach for the characterization of transport and optical properties of aerosol particles near sources Part I: Measurement of particle backscatter coefficient maps with a scanning UV Lidar. *Atmos. Environ.* **2011**, *45*, 2795–2802.

16. Deuzé, J.L.; Bréon, F.M.; Devaux, C.; Goloub, P.; Herman, M.; Lafrance, B.; Maignan, F.; Marchand, A.; Nadal, F.; Perry, G.; *et al*. Remote sensing of aerosols over land surfaces from POLDER-ADEOS-1 polarized measurements. *J. Geophys. Res. Atmos.* **2001**, *106*, 4913–4926.

17. Dubovik, O.; Herman, M.; Holdak, A.; Lapyonok, T.; Tanre, D.; Deuze, J.L.; Ducos, F.; Sinyuk, A.; Lopatin, A. Statistically optimized inversion algorithm for enhanced retrieval of aerosol properties from spectral multi-angle polarimetric satellite observations. *Atmos. Meas. Tech.* **2011**, *4*, 975–1018.

18. Hasekamp, O.P.; Litvinov, P.; Butz, A. Aerosol properties over the ocean from PARASOL multiangle photopolarimetric measurements. *J. Geophys. Res.* **2011**, *116*, doi:10.1029/2010JD015469.

19. Eck, T.F.; Holben, B.N.; Sinyuk, A.; Pinker, R.T.; Goloub, P.; Chen, H.; Chatenet, B.; Li, Z.; Singh, R.P.; Tripathi, S.N.; *et al*. Climatological aspects of the optical properties of fine/coarse mode aerosol mixtures. *J. Geophys. Res. Atmos.* **2010**, *115*, doi:10.1029/2010JD014002.

20. Che, H.Z.; Xia, X.G.; Zhu, J.; Hong, W.; Wang, Y.Q.; Sun, J.Y.; Zhang, X.Y.; Shi, G.Y. Aerosol optical properties under the condition of heavy haze over an urban site of Beijing, China. *Environ. Sci. Pollut. Res.* **2015**, *22*, doi:10.1007/s11356-014-3415-5.

21. Jing, J.S.; Wu, Y.F.; Tao, J.; Che, H.Z.; Xia, X.G.; Zhang, X.C.; Yan, P.; Zhao, D.M.; Zhang, L.M. Observation and analysis of near-surface atmospheric aerosol optical properties in urban Beijing. *Particuology* **2015**, *18*, doi:10.1016/j.partic.2014.03.013.

22. Lac, C.; Donnelly, R.P.; Masson, V.; Pal, S.; Riette, S.; Donier, S.; Queguiner, S.; Tanguy, G.; Ammoura, L.; Xueref-Remy, I. CO_2 dispersion modelling over Paris region within the CO_2-MEGAPARIS project. *Atmos. Chem. Phys.* **2013**, *13*, 4941–4961.

23. Pal, S.; Xueref-Remy, I.; Ammoura, L.; Chazette, P.; Gibert, F.; Royer, P.; Dieudonné, E.; Dupont, J.-C.; Haeffelin, M.; Lac, C.; *et al*. Spatio-temporal variability of the atmospheric boundary layer depth over the Paris agglomeration: An assessment of the impact of the urban heat island intensity. *Atmos. Environ.* **2012**, *63*, 261–275.

24. Flowerdew, R.J.; Haigh, J.D. An approximation to improve accuracy in the derivation of surface reflectances from multi-look satellite radiometers. *Geophys. Res. Lett.* **1995**, *22*, 1693–1696.

25. Flowerdew, R.J.; Haigh, J.D. Retrieval of aerosol optical thickness over land using the ATSR-2 dual-look satellite radiometer. *Geophys. Res. Lett.* **1996**, *23*, 351–354.

26. North, P.R.J. Estimation of aerosol opacity and land surface bidirectional reflectance from ATSR-2 dual-angle imagery: Operational method and validation. *J. Geophys. Res.* **2002**, *107*, 4149.

27. Evans, K.F.; Stephens, G.L. A new polarized atmospheric radiative-transfer model. *J. Quant. Spectrosc. Radiat. Transf.* **1991**, *46*, 413–423.

28. Diner, D.J.; Martonchik, J.V.; Kahn, R.A.; Pinty, B.; Gobron, N.; Nelson, D.L.; Holben, B.N. Using angular and spectral shape similarity constraints to improve MISR aerosol and surface retrievals over land. *Remote Sens. Environ.* **2005**, *94*, 155–171.

29. Bréon, F.M.; Colzy, S. Cloud detection from the spaceborne POLDER instrument and validation against surface synoptic observations. *J. Atmos. Sci.* **1999**, *38*, 777–785.

30. Nadal, F.; Bréon, F.M. Parameterization of surface polarized reflectance derived from POLDER spaceborne measurements. *IEEE Trans. Geosci. Remote* **1999**, *37*, 1709–1718.

31. Yu, X.N.; Zhu, B.; Zhang, M.G. Seasonal variability of aerosol optical properties over Beijing. *Atmos. Environ.* **2009**, *43*, 4095–4101.

32. Wang, S.; Fang, L.; Gu, X.; Yu, T.; Gao, J. Comparison of aerosol optical properties from Beijing and Kanpur. *Atmos. Environ.* **2011**, *45*, 7406–7414.

33. Dubovik, O.; Sinyuk, A.; Lapyonok, T.; Holben, B.N.; Mishchenko, M.; Yang, P.; Eck, T.F.; Volten, H.; Munoz, O.; Veihelmann, B.; *et al*. Application of spheroid models to account for aerosol particle nonsphericity in remote sensing of desert dust. *J. Geophys. Res. Atmos.* **2006**, *111*, doi:10.1029/2005JD006619.

34. Holben, B.N.; Eck, T.F.; Slutsker, I.; Tanre, D.; Buis, J.P.; Setzer, A.; Vermote, E.; Reagan, J.A.; Kaufman, Y.; Nakajima, T.; *et al*. AERONET—A federated instrument network and data archive for aerosol characterization. *Remote Sens. Environ.* **1998**, *66*, 1–16.

35. Holben, B.N.; Tanré, D.; Smirnov, A.; Eck, T.F.; Slutsker, I.; Abuhassan, N.; Newcomb, W.W.; Schafer, J.S.; Chatenet, B.; Lavenu, F.; *et al*. An emerging ground-based aerosol climatology: Aerosol optical depth from AERONET. *J. Geophys. Res.* **2001**, *106*, 12067–12097.

36. Bréon, F.M.; Vermeulen, A.; Descloitres, J. An evaluation of satellite aerosol products against sunphotometer measurements. *Remote Sens. Environ.* **2011**, *115*, 3102–3111.